This PhD thesis was elaborated at the Department of Cellular and Molecular Neuroendocrinology of the Institute of Physiology, Academy of Sciences of the Czech Republic, Prague. It is a completion of PhD studies of Biomedicine at the 1st Faculty of Medicine, Charles University in Prague, specialization Neurosciences.

Commission: Neurosciences

Chairman of the Commission: Prof. MUDr. J. Šonka, DrSc.

Applicant: Marie Jindrichova
Institute of Physiology, AS CR, vvi
Videnska 1083
142 20 Prague 4
Czech Republic
Phone: +420 776 887 852
Email: jindrichova@biomed.cas.cz

Supervisor: Hana Zemkova, RNDr., CSc.
Institute of Physiology, AS CR, vvi
Videnska 1083
142 20 Prague 4
Czech Republic
Phone: +420 776 887 852
Email: zemkova@biomed.cas.cz

Opponents:

Summary was sent out on:

Defence of the Thesis:

Table of Contents

1. Summary

Purinergic P2X receptors are a family of ligand-gated cationic channels activated by extracellular ATP (adenosine-5´-triphosphate). They play a role in neurotransmission, pain sensation, modulation of neurotransmitter and hormone release and many other physiological and pathophysiological processes. Little is known about their structure, mechanism of channel opening, localization and role in the central nervous system.

A single P2X receptor subunit is composed of intracellular N- and C-termini, two transmembrane domains (TM1 and TM2) and large extracellular loop. There are seven mammalian P2X subunits, called P2X1-7, which all share similar topology but vary in sensitivity to agonists, antagonists and allosteric modulators. The P2X4 subtype is the only mammalian purinergic receptor which is sensitive by extracellularly applied ivermectin (IVM), a large macrocyclic lipophilic substance. IVM specifically enhances the P2X4 receptor-channel function by interacting with TM domains in the open conformation state. We used cysteine-scanning mutagenesis of the rat P2X4 receptor and electrophysiological recording to identify residues of potential importance for interaction with IVM, the ATP binding and/or channel gating mechanism, and to establish the secondary structure of TMs. Residues Arg^{33}, Gln^{36}, Leu^{40}, Val^{43}, Val^{47}, Trp^{50}, Asn^{338}, Gly^{342}, Leu^{346}, Ala^{349}, Cys^{353} and Ile^{356} can be considered as IVM-sensitive hits. The pattern of these 12 residues was consistent with helical structure of both TMs, with every third or fourth amino acid affected by substitution. They lie on the same side of their TM helices, and could face lipids in the open conformation state and provide the binding pocket for IVM. In contrast, the IVM-independent hits Met^{31}, Tyr^{42}, Gly^{45}, Val^{49}, Gly^{340}, Leu^{343}, Gly^{347}, Thr^{350}, Asp^{354}, Val^{357} map the opposite side of their helices, probably facing the protein of neighbouring P2X subunit or pore of the channel, and play important roles in channel gating.

Next we performed detailed analysis of functional role of aromatic residues in the upper part of TM1 of several P2X receptors. Replacement of conserved tyrosine residue with alanine had a receptor specific effect: the P2X1 receptor was nonfunctional, the P2X2 and P2X4 (and to smaller extend the P2X3) receptors exhibited enhanced sensitivity to ATP and α,β-meATP accompanied with prolonged deactivation. The P2X7 receptor function was not affected. At P2X4 receptor, replacement of conserved Tyr^{42} with other amino acids also enhanced the receptor sensitivity to agonist and delayed deactivation in order: Gly > Ile > Ala > Cys > Trp > Phe > Tyr; logarithmic plot showed a strong inverse

relationship between the EC_{50} and deactivation time constant values. Alanine substitution of several other aromatic residues in the upper part of TM1 domain in the P2X2, P2X3, and P2X4 receptors also altered agonist sensitivity and the deactivation time constant but this effect was smaller than that observed in the TM1 tyrosine mutants. The function of P2X4-Y42A mutant, could be restored by replacement of Trp^{46} and Trp^{50} residues with alanine, whereas mutation of aromatic Phe^{48} residue and non-aromatic Val^{43} and Gly^{29} residues was ineffective. These results indicate that conserved tyrosine and nearby aromatic residues in the upper part of TM1 play important roles in three-dimensional structure of P2X receptors and are required for agonist binding and/or channel gating.

2. Introduction

Purinergic P2X receptors (P2XRs) are ATP-gated channel, which allow the entry of Ca^{2+} in addition to monovalent cations such as Na^{+} and K^{+}, and small organic cations (Valera et al., 1994). In vertebrates, seven genes encode P2X receptor subunits (termed P2X1--7), which are 26-47 % identical in amino acids sequence (Khakh et al., 2001). P2XRs are organized as trimeric homomers or heteromers (Nicke et al., 1998). All subunits have two transmembrane domains (TM1 and TM2), linked by a large extracellular loop containing the ATP binding site, and intracellular N- and C- termini (Brake et al., 1994; Valera et al., 1994). The TM domains form the pore of P2X channel; the TM1 domain is positioned more peripherally than TM2 (Li et al., 2008). Both TM1 and TM2 are predicted to adopt α-helix structures in activated P2X2R (Rassendren et al., 1997; Egan et al., 1998; Haines et al., 2001; Jiang et al., 2001; Migita et al., 2001; Li et al., 2004; Khakh and Egan, 2005) and the same prediction exists for TM1 of the P2X4R (Silberberg et al., 2005). The TM domains of different subunits move relative to each other during channel opening and closing; mainly in their upper parts: Tyr^{42}-Val^{47} of TM1 and Thr^{335}-Leu^{346} of TM2 (P2X4 numbering) (Egan et al., 1998; Jiang et al., 2001; Li et al., 2004; Silberberg et al., 2005). The TM2 domain appears to play a dominant role in receptor functions, including channel assembly, gating, ion selectivity, and the permeability for divalent ions (Egan et al., 1998; Migita et al., 2001; Egan and Khakh, 2004; Li et al., 2004; Khakh and Egan, 2005; Samways and Egan, 2007; Li et al., 2008). The TM2 residues Thr^{336}, Thr^{339} and Ser^{340} were suggested to contribute to formation of the pore, gate and selective filter at the P2X2R (Migita et al., 2001; Egan and Khakh, 2004; Samways and Egan, 2007; Li et al., 2008). The TM1 domain seems to be less important for control of ion fluxes (Jiang et al., 2003; Khakh and Egan, 2005; Samways et al., 2008), but together with TM2 domain contributes to the control of Ca^{2+} influx (Samways et al., 2008) and to transition of the channel pore from relatively selective to the dilated state (Khakh and Egan, 2005). The TM1 domain may also play a role in receptor sensitivity to agonists. For example, replacement of the TM1 domain of the rat P2X2 subunit with one from α,β--meATP-sensitive subunits (P2X1 or P2X3) converted the resulting chimera to α,β-meATP sensitivity (Haines et al., 2001). What aspects of structure and/or dynamics of TM1 give rise to this change in sensitivity is unknown.

The P2X4R displays a number of similarities to the P2X2R and falls into the category of moderate desensitizing P2X receptors. P2X4R cDNAs were independently isolated by five

different groups of investigators from various rat tissues and have more recently been isolated from human, mouse, chick and *Xenopus* (for review see North, 2002). The P2X4R is the only mammalian purinergic receptor which is modulated by extracellularly applied ivermectin (IVM). IVM is a member of class of lipophilic compounds known as avermectins and is used as an antiparasitic agent. The therapeutic effect of IVM is believed to be mediated by an interaction of this compound with glutamate-gated chloride channels expressed by parasite, leading to muscle paralysis and starvation (Cully et al., 1994; Dent et al., 1997). IVM modulate several other ligand-gated channels, including $GABA_A$ receptors from chick and mouse (Sigel and Baur, 1987; Krusek and Zemkova, 1994), recombinant glycine--activated chloride channels (Shan et al., 2001), and neuronal α7nicotinic receptors from chick and human (Krause et al., 1998). IVM is a relatively large molecule ***(Fig. 1)***, spanning a distance of about 20 Å (Albers-Schonberg et al., 1981; Hu et al., 1998).

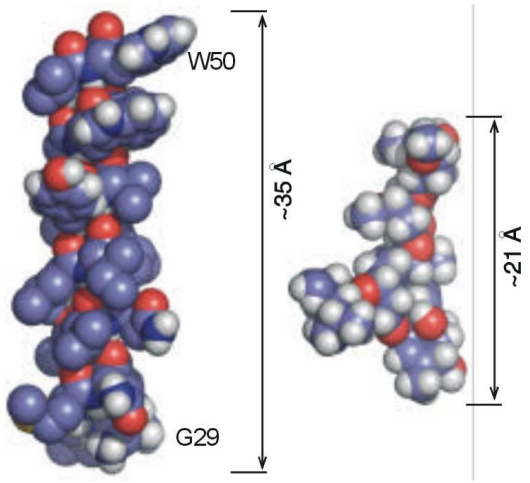

Fig. 1 Models of TM1 helix of P2X4R and IVM:

Schematic comparison of the sizes of the TM1 segment of P2X4R modeled as regular α-helix (*left*) and IVM molecule (*right*). The TM1 model started with the Gly^{29} residue and ended with the Trp^{50} residue, the first located in extracellular loop.

IVM acts on the P2X4R channels as an allosteric modulator; it increases sensitivity to agonists, potentiates maximum current amplitude and prolongs deactivation kinetics of the channel after agonist washout (Khakh et al., 1999; Priel and Silberberg, 2004). IVM enhances the P2X4R-channel function by binding between two TM domains (Silberberg et al., 2007) and stabilizes the open conformation state of the P2X4 channel (Priel and Silberberg, 2004). The exact topology of its binding site has not yet been described.

We focused on identification of the P2X4R transmembrane residues contributing to the effects of IVM and we also used IVM as a pharmacological tool for studying the TMs and the pore channel structures.

The upper parts of P2XR-TM1 domains are enriched with aromatic residues ***(Fig. 2)***. In addition to the conserved tyrosine at α-position, phenylalanine at β-position is present in the P2X2R and P2X3R, homologous aromatic residues Trp/Tyr/Phe at γ-position are conserved in all receptors, and phenylalanine at δ-position is present in five of seven receptors.

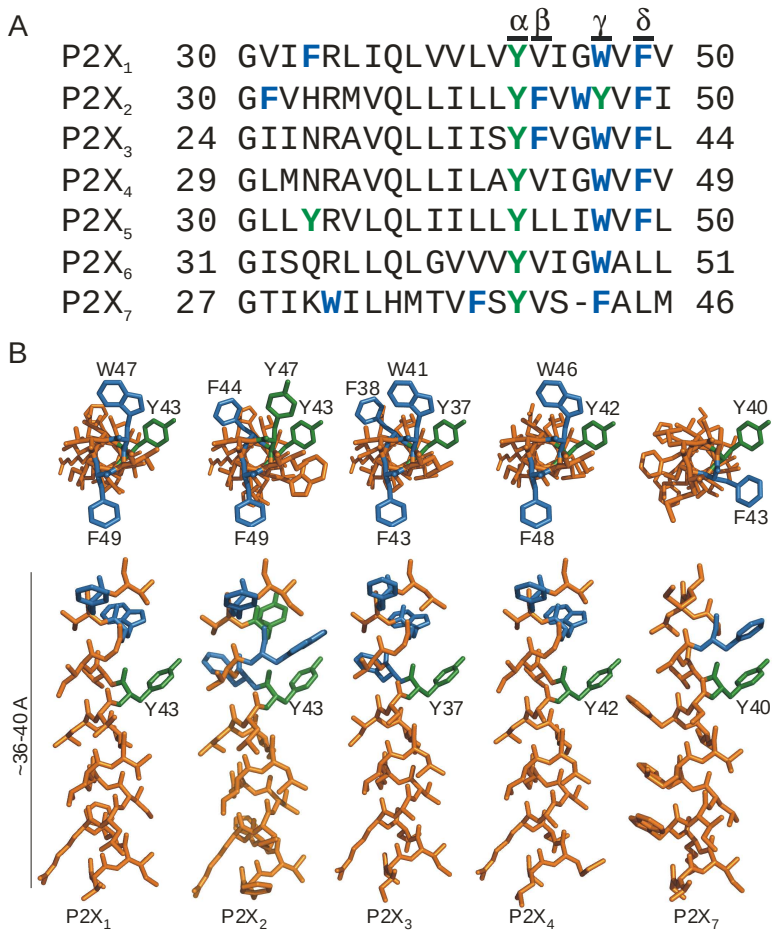

Fig. 2 Positions of aromatic residues in TM1 domains of rat P2XRs:

(A) Alignment of amino acid sequences of the first transmembrane domain (TM1) of seven rat P2X receptors (P2X1-7). Aromatic residues are shown in *green* (polar) and *blue* (nonpolar). α-δ indicates positions of aromatic residues in the upper part of TM1 domain. (B) Three-dimensional models of predicted α-helical TM1 segments of P2X1R, P2X2R, P2X3R, P2X4R, and P2X7R. The models started with the Gly^{29} residue and ended with the Val^{49} residue (P2X4 receptor numbering). Helical models viewed from the extracellular side (*top*) and from the membrane (*bottom*) with aromatic residues in α-δ positions (green and blue) are shown.

The results of alanine scanning mutagenesis of the P2X2R showed that aromatic residues in this part of TM1 (Tyr^{43} and Phe^{44}) play an important role in receptor functions. Their substitution generates a low-responsive channels with enhanced sensitivity to agonists (Haines et al., 2001; Li et al., 2004). The second aim of our study was to provide a comparative view on the role of TM1 aromatic residues in receptor functions, using for this purpose the rat P2X1, P2X2, P2X3, P2X4, and P2X7 receptors expressed in HEK293 cells.

3. Experimental Questions

The general aim of this Thesis was to contribute to understanding the relationship between the structure and function of the rat purinergic P2XR transmembrane domains with using alanine and cysteine scanning mutagenesis, electrophysiological technique of patch clamp recording and transfected HEK293 cells. The specific aims were to:

1. Identify the TM1 and TM2 residues of the P2X4R that are important for modulatory effect of IVM.
2. Determine TM1 and TM2 residues that are important for gating of the P2X4R channel and solve the question whether or not both TM domains of the P2X4R adopt α-helical structure.
3. Clarify the role of TM1 conserved tyrosine in the mechanism of channel gating and receptor sensitivity to agonists across several P2X receptors.
4. Examine substitution of conserved TM1 tyrosine with amino acids of different physical and chemical properties.
5. Analyze the contribution of aromatic residues in the upper part of TM1 in several P2XRs to the receptor-specific sensitivity to agonists and channel gating properties.

4. Materials and Methods

4.1 DNA constructs

cDNAs encoding the sequences of the rat P2X1, P2X2, P2X3, P2X4, P2X7 wild type and mutated receptors were subcloned into the biscistronic enhanced fluorescent protein expression vector, pIRES2-EGFP (Clontech, Mountain View, CA). Single-point mutant P2X receptors were constructed by PCR amplification using specific overlapping oligonucleotide primers (synthesized by VBC-genomics, Vienna, Austria), QuikChange II site-directed mutagenesis kit (Stratagene, La Jolla, CA) and P2X/pIRES2-EGFP as the template. The C-terminal EGFP tagged P2X4 construct was also used for mutagenesis. Previous experiments showed that this receptor respond to ATP with the same sensitivity and peak amplitude of current highly comparable to that observed in cells expressing non-tagged wild type (WT) receptor (Yan et al., 2005). Plasmid DNAs for transfection were purified using a Jetquick plasmid spin kit (Genomed, Löhne, Germany). The presence of the mutations was confirmed by automated DNA sequencing (ABI Prism 3100 Genetic Analyzer, Applied Biosystems, Foster City, CA, performed by the Laboratory of DNA sequencing, Institute of Microbiology, ASCR, Prague).

4.2 Cells cultures and transfection

Experiments were performed on human embryonic kidney 293 cells (HEK293; American Type Culture Collection), which were grown in Dulbecco's modified Eagle's medium (Invitrogen, Carlsbad, CA, USA) supplemented with 10% fetal bovine serum, 50 U/ml penicillin and 50 μg/ml streptomycin in a humidified 5% CO_2 atmosphere at 37 °C. Cells were cultured in 75 cm^2 plastic culture flasks (NUNC, Rochester, NY) for 36-72 h until they reached 80-95% confluence. The day before transfection, the cells were plated on poly--L-lysine coated cover slips in a 35 mm culture dishes (Sarstedt, Newton, NC) at density ~150,000 cells/dish and incubated at 37 °C for at least 24 h. Transient transfection of the cells was carried out using either WT or mutant cDNA (1 μg) and Lipofectamine2000 (7 μl) in 2 ml of serum-free OptiMEM. After 4-6 hr of incubation, the transfection mixture was replaced with normal culture medium. The experiments were performed 24 - 48 hr after transfection.

4.3 Patch clamp recordings

Currents were recorded in a whole-cell configuration from cells clamped to -60 mV using Axopatch 200B patch-clamp amplifier (Axon Instruments, Union City, CA). All currents were captured and stored using Digidata 1200 and pClamp8.0 software package (Axon Instruments, Union City, CA). Patch electrodes were pulled from a glass tube with a 1.65 mm outer diameter on horizontal puller (model P-97, Sutter Instruments, Novato, CA). The tip of the pipette was heat-polished and its resistance was 3-5 MΩ. During the experiments, the dishes with cell cultures were continuously perfused with an extracellular solution containing (in mM): 142 NaCl, 3 KCl, 2 $CaCl_2$, 1 $MgCl_2$, 10 HEPES and 10 D--glucose, adjusted to pH 7.3 with 1M NaOH. The osmolarity of solution was 290 – 300 mOs/l as determined by a vapor pressure osmometer (Model Vapro 5520; Wescor, Logan, UT). Patch electrodes used for whole-cell recording were filled with an intracellular solution containing (in mM): 154 CsCl, 11 EGTA, and 10 HEPES; pH was adjusted with 1 M CsOH to 7.2. The osmolarity of intracellular solution was 280 – 290 mOs/l. IVM was dissolved in DMSO, stored in stock solutions at 0.01 M, and diluted to required concentration in extracellular solution prior to experiments. Control and ATP-containing solutions were applied using RSC-200 Rapid Solution Changer system (BIO-LOGIC, Claix, France). Brief application (2-5 s duration, 2-3 min interval) of different concentrations of agonists was used to evoke inward current. Experiments were carried out at room temperature (RT).

4.4 Calculations

Dose-response data points were fitted by a three-parameter logistic equation using a nonlinear curve-fitting program that derives the EC_{50} and Hill coefficient values of the produced curves (SigmaPlot 2000 v9.01; SPSS Inc., Chicago, IL). The form of the fitted equation was $y=I_{max}/(1 + (EC_{50}/x)^{n_H}$, where y is the amplitude of the current evoked by ATP, I_{max} is the maximum current amplitude induced by 100 μM ATP, EC_{50} is the agonist concentration producing 50% of the maximal response, n_H is the Hill coefficient, and x is the concentration of ATP. The kinetics of current decay evoked by washout of agonists, termed deactivation, were fitted by a single exponential function [$y=A_1\ exp(-t/tau)$] or by the sum of two exponentials [$y=A_1\ exp(-t/tau_1) + A_2\ exp(-t/tau_2)$] using the program Clampfit v.9 (Axon Instruments, Union City, CA), where A_1 and A_2 are relative amplitudes of the first and second exponential, and tau_1 and tau_2 are time constants. The derived time constant for deactivation was labeled as τ_{off}. All numerical values in the text are reported

as mean ± SEM. Significant differences, with $P<0.01$, were determined by one-way analysis of variance using SigmaStat 2000 v9.01.

4.5 Localization of EGFP-tagged receptors

HEK293 cells expressing P2X4-WT or mutants P2X4-Y42R, -Y42D tagged with EGFP plated onto 12 mm poly-L-lysine cover slips, were fixed in ice-cold 4% paraformaldehyde in PBS (pH 7.2) for 5 min, dehydrated through ascending set of ethanol (70 %, 80 %, 95 %, 1 min in each) and coverslips mounted in Vectashield medium (Vector Laboratories, Burlingame, CA).

To test the presence of P2X1 proteins in the membrane imunocytochemistry was used. After fixation the cells were incubated in Phosphate Buffered Saline (PBS) (pH 7.2) containing 2 % donkey serum plus 0.05 % Tween 20, 1 % BSA and 0.1 % Triton for 20 min, then with primary rabbit anti-P2X1R antibody (1:200) for 1 hr in RT (Alomone Labs, Jerusalem, Israel). Then washed three times for 5 min in the PBS solution and incubated with secondary fluorescein-conjugated donkey anti-rabbit antibody for 1 hr (Jackson Immuno Research, Baltimore, Baltimore, PA). After intensive washing, the cultures dehydrated and covered with Vectashield medium. The localization of P2X receptors in cells was examined by laser scanning confocal microscopy (Leica SP2 AOBS, Germany). Images were collected under 60x objective lens with applying further zoom.

4.6 Helical wheel projection and 3D modeling

Helical wheel projections of TM domains of P2X4R were created using the internet-based application at http://cti.itc.virginia.edu/~cmg/Demo/wheel/wheelApp.html. Molecule model of ivermectin was created by Doc. RNDr. Tomas Obsil, PhD. (Department of Protein Structure, Academy of Sciences of the Czech Republic, Prague) with using software Ghemical (Hassinen and Perakyla, 2001) and program Desktop Molecular Modeller v4.2 (Polyhedron software, Witney, UK). Helical models of TM1 domains P2X1-7R by using DeepView/Swiss-PdbViewer v3.7 (Guex and Peitsch, 1997) and PyMol v0.99 (http://www.pymol.org).

5. Results

To identify TM residues of the P2X4R with the potential importance for interactions with IVM and channel gating we performed scanning cysteine mutagenesis of TM1 (residues Gly^{29}-Trp^{50}) and TM2 domain (Asn^{338}-Leu^{358}). Wild type (WT) and mutated receptors were expressed in HEK293 cells and whole-cell patch clamp recording was used to measure channel activity with focusing on following parameters: the molar concentration of ATP required to produce 50% of the maximal current (EC_{50}), the peak current amplitude in response to the supramaximal agonist concentration (I_{max}) and the rates of current decay after washout of agonist (τ_{off}), which reflected deactivation kinetics (all in the absence and presence of IVM). As a main indicator of IVM effects we used changes in τ_{off} because this parameter of current is not dependent on agonist concentration (Zemkova et al., 2007).

The majority of TM1 (16 of 22) and TM2 (13 of 21) cysteine mutants showed no significant changes in receptor function in the absence of IVM: L30C, N32C, A34C, V35C, Q36C, L37C, L38C, I39C, L40C, A41C, V43C, I44C, W46C, V47C, F48C, W50C, N338C, V339C, G342C, A344C, L345C, L346C, V348C, A349C, V351C, L352C, V355C, L356C, and L358C ***(Fig. 3, 4)***. Among these mutants, the IVM effects were weakened at Q36C, L40C, V43C, V47C, W50C, N338C, G342C, L346C and A349C mutants and strengthened at the I356C mutant. The changes in IVM effect at these mutants illustrate the relevance of residues for the interaction with IVM.

Cysteine mutants showing significant changes in receptor function in the absence of IVM could be divided into following subgroups: (i) The S341C, G347C, T350C and V357C mutants showed significantly lower I_{max} responses, but their EC_{50} values were comparable to the WT receptor. (ii) Mutants with significant shifts in the EC_{50} values: The R33C, M31C, L343C, C353A mutants showed decreased sensitivity to ATP; the G45C, Y42C and G340C mutants exhibited enhanced sensitivity. (iii) Mutants with low ATP responsiveness (V49C and G29C) and silent mutation (D354C). Changes of the P2X4R kinetics after substitution suggest the important role of these residues in the receptor functions. But it was reasonable to include the residues Arg^{33} and Cys^{353} into IVM-sensitive hits, because the parallelism between their EC_{50} values and rates of current deactivation (Zemkova et al., 2007) was lost.

P2X4R	-IVM EC_{50} (μM)	+IVM EC_{50} (μM)	-IVM I_{max} (nA)	+IVM I_{max} (nA)	-IVM τ_{off} (s)	+IVM τ_{off} (s)
WT	4.6±0.3	0.5±0.1	1.6±0.2	2.8±0.2	0.4±0.04	26±1.6
W50C	7.3±1.9	2.2±0.1*	1.6±0.4	2.5±0.3	0.5±0.20	4±0.4*
V49C[a]	n.d.	1.8±0.3*	0.3±0.1*	0.9±0.3*	0.4±0.05	15±1.9*
F48C	3.8±1.3	0.5±0.2	1.2±0.3	1.9±0.3	0.4±0.1	31±2.8
V47C	3.6±1.2	1±0.1	1.3±0.2	2±0.1*	0.3±0.01	16±1.6*
W46C	6.2±0.2	0.4±0.1	1±0.2	1.4±0.3*	0.5±0.16	26±2.7
G45C	1.6±0.3*	0.2±0.03	1.8±0.3	2.9±0.5	0.4±0.04	76±9.3*
I44C	4.1±0.4	0.4±0.03	2.1±0.5	2.6±0.3	0.3±0.03	31±4.6
V43C	4.5±0.5	2.2±0.4*	1.4±0.4	2.2±0.5	0.3±0.15	2.7±0.5*
Y42C[b]	0.6±0.1*	0.5±0.1	0.5±0.2*	0.4±0.2*	21±1.8*	32±4.2
A41C	5.1±0.8	0.7± 0.4	1.6±0.3	2.4±0.2	0.3±0.05	26±2.9
L40C	7.2±1.2	1.7±0.5*	1.2±0.1	2.7±0.2	0.2±0.09	13±1.3*
I39C	4.6±1.3	0.5±0.1	1.3±0.3	2.1±0.4	0.2±0.18	30±3.6
L38C	7.4±2.5	0.9±0.1	1.8±0.2	2.4± 0.4	0.2±0.03	19±2.1
L37C	6.3±0.7	0.9±0.2	1.8±0.9	2.3±0.2	0.3±0.05	22±2.5
Q36C	7.4±2.5	1.9±0.2*	1.4±0.2	2.5±0.4	0.2±0.03	13±2.0*
V35C	4.1±1.0	0.6±0.3	1.5±0.2	2±0.5	0.3±0.04	37±3.2
A34C	3.9±1.1	0.5±0.5	2.0±0.4	2.5±0.4	0.3±0.05	24±2.1
R33C	9.9±1.8*	2.9±1.4*	0.6±0.1*	0.8±0.2*	0.7±0.2	22±2.8
N32C	6±0.9	0.8±0.1	2±0.3	2.8±0.4	0.4±0.07	20±4.7
M31C[a]	15±2*	1±0.2	1.1±0.2	2.6±0.3	0.3±0.15	17±2.5*
L30C	5.7±0.7	0.9±0.2	1.3±0.3	2.6±0.4	0.3±0.02	21±3.0
G29C[a]	n.d.	4.9±0.7*	0.1±0.05*	0.5±0.1*	0.3±0.02	16±1.3*

Fig 3 Ivermectin (IVM) effects on wild type (WT) and transmembrane-1 mutants of P2X4 receptors:

EC_{50}, ATP concentration producing 50% of the maximal current response; I_{max}, maximum amplitude of current induced by 100 μM ATP; τ_{off}, deactivation time constant of currents after removal ATP; n.d., not determined. Each receptor was examined in 5 to 29 cells in the presence (+IVM) or absence (-IVM) of 3 μM IVM. Control WT data are pooled from cells expressing wild-type P2X4 receptor tested in each experiment. [a]1 mM ATP was used to estimate I_{max}. [b]τ_{off} in the absence of IVM for this mutant was 21±1.8 s and did not differ from τ_{des} estimated during the prolonged agonist application. (*) $P<0.01$ between WT and mutants.

P2X4R	-IVM EC_{50} (μM)	+IVM EC_{50} (μM)	-IVM I_{max} (nA)	+IVM I_{max} (nA)	-IVM τ_{off} (s)	+IVM τ_{off} (s)
WT	4.6±0.3	0.5±0.1	1.6±0.2	2.8±0.2	0.4±0.1	26±1.6
N338C	4.6±0.8	2.5±1.1*	1±0.3	2.4±0.3	0.5±0.1	1.9±0.1*
V339C	3.8±0.2	0.7±0.1	2.3±0.4	3.4±0.5	0.6±0.1	27±0.4
G340C[a]	0.7±0.1*	0.6±0.2	0.8±0.2*	0.9±0.2 *	3.8±0.3*	15±1.5*
S341C[b]	6±1.1	1.8±0.5*	0.5±0.1*	1.3±0.2*	0.6±0.1	12±1.4*
G342C	3.1±0.5	2.2±0.5*	1.4±0.2	2.8±0.3	1.7±0.2*	3.8±0.5*
L343C[b]	>100	15±2.6*	1.6±0.3	2.7±0.3	0.7±0.1	4.2±0.5*
A344C[c]	3.4±0.5	n.d.	1.3±0.3	n.d.	0.7±0.1	26±3.7
L345C	6.5±1.7	1±0.4	1.8±0.5	2.8±0.4	0.9±0.3	19±2.1
L346C	3.3±0.7	2.1±0.5*	1.5±0.3	2.7±0.4	0.8±0.2	4.3±1.2*
G347C	7.5±0.4	0.8±0.2	0.5±0.1*	2.4±0.4	0.6±0.1	20±2.9
V348C	3.2±0.6	0.7±0.2	1.7±0.5	3±0.3	0.7±0.1	22±1.8
A349C	4.5±0.5	1.4±0.4*	1.1±0.3	2.3±0.4	0.4±0.1	10±1.5*
T350C	4.8±1	0.7±0.5	0.9±0.2*	1.8±0.3*	0.7±0.1	34±3.3
V351C	5.1±0.7	1.3±0.2*	1.4±0.3	2.7±0.4	0.5±0.04	19±1.9
L352C	5.5±1.2	0.7±0.1	1.1±0.2	2.3±0.2	0.4±0.1	20±3.1
C353A	10±3.2*	2.3±1.1*	0.7±0.1*	1.3±0.4*	0.2±0.05	24±2.5
D354C[d]	-	-	-	0.1±0.05*	-	n.d.
V355C	4.7±1.5	0.7±0.2	1.2±0.5	1.8±0.2*	0.4±0.04	21±2.2
I356C	4.4±1.2	0.8±0.1	1.2±0.5	2.2±0.4	0.3±0.03	51±7.1*
V357C	3.2±1.3	0.5±0.3	0.6±0.1*	1.5±0.2*	0.4±0.07	34±1.4
L358C	2.5±1.6	0.6±0.2	1.2±0.1	1.7±0.2*	0.3±0.07	30±2.2

Fig 4 Characterization of IVM effects on transmembrane-2 mutants of P2X4 receptors:

Each receptor was examined in 7 to 17 cells in the presence (+IVM) or absence (-IVM) of 3 μM IVM. [a]Prolonged desensitization of receptor after washout of agonist contributes to τ_{off} value in the absence of IVM (3.8±0.3 s). [b]1 mM ATP was used to estimate I_{max}. [c]The EC_{50} and I_{max} values in the presence of IVM could not be examined in the same cells in the absence and presence of IVM because of rapid run-down of current and τ_{off} value of the mutant represents the slow component derived from two-exponential fitting. [d]3 mM ATP was used to estimate I_{max}. (*) $P<0.01$ between WT and mutants.

The pattern of IVM-sensitive hits (Arg^{33}, Gln^{36}, Leu^{40}, Val^{43}, Val^{47}, Trp^{50} of TM1 and Asn^{338}, Gly^{342}, Leu^{346}, Ala^{349}, Cys^{353}, Ile^{356} of TM2) is consistent with a helical secondary structure, in which every third or fourth residue was affected by substitution, and these residues line the same side of the predicted helices ***(Fig. 5)***. Such a pattern is also consistent with the hypothesis that these residues face lipids in the open conformation state and contribute to the formation of the binding pocket for IVM. The *Schistosoma mansoni* P2X receptor is also IVM sensitive, although residues of helices are only 52% identical with the P2X4 subunit. However, 11 out of 12 residues that we identified as IVM hits are also present in this receptor, and the residue Trp^{50} is substituted with tyrosine. Among rat P2XR subunits, eight residues are also present in the P2X1, in other subunits this number is between three and seven.

Scanning mutagenesis of TM domains of P2X4 revealed substitution-sensitive residues (Gly^{29}, Met^{31}, Tyr^{42}, Gly^{45}, Val^{49}, Trp^{50} of TM1 and Gly^{340}, Ser^{341}, Leu^{343}, Ala^{344}, Gly^{347}, Thr^{350}, Asp^{354}, Val^{357} of TM2) with important role in receptor functions other than coordination of the IVM molecule. All these residues (except Gly^{29} and Ser^{341}) map another side of the α-helix of TM domains than IVM hits and, thus, could face the protein or hydrophilic pore ***(Fig. 5)***.

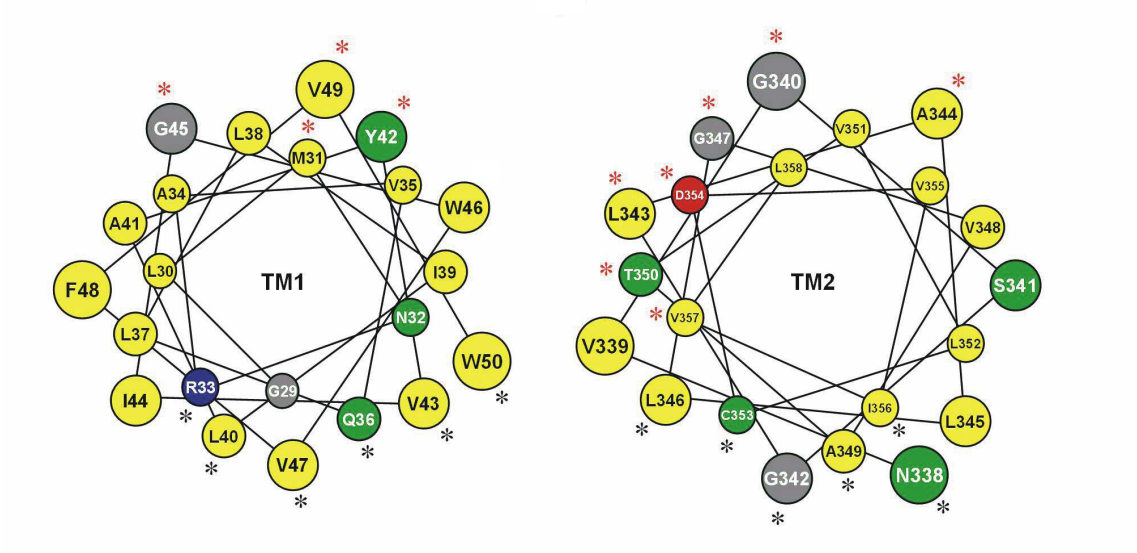

Fig. 5 Helical wheel projection of TM1 and TM2 domains of P2X4 receptor:

The predicted α–helical structure of the TM1 segment consisting of 22 amino acids (from Gly^{29} to Trp^{50}) and TM2 segment consisting of 21 amino acids (from Asn^{338} to Leu^{358}) viewed from the extracellular side of the membrane. Black asterisks indicate amino acid residues showing altered sensitivity to IVM and red asterisks indicate residues showing IVM-independent changes in receptor

function. Colors of circles indicate glycine (*gray*), hydrophobic nonpolar (*yellow*), polar uncharged (*green*), basic (*blue*) and acidic residue (*red*).

Alanine scanning mutagenesis of P2X4R-TM1 domain showed comparable results with cysteine scanning. The substitution-insensitive mutants were L30A, N32A, A34F, V35A, L37A, L38A, I39A, A41L, I44A, W46A and F48A. In the absence of IVM, the receptor function was also not affected in mutants L40A, V43A, V47A, W50A, but these receptors showed significant changes in the EC_{50} values for ATP and deactivation kinetics in the presence of IVM compared to the P2X4R-WT suggested them as IVM-sensitive hits. The same four residues were also identified as IVM-sensitive hits after cyteine scanning mutagenesis. Results support the helical organization of the upper part of TM1 domain in activated P2X4 receptor and the potential role of some residues in IVM binding. The only difference was that Q36C mutant was recognized as an IVM-sensitive mutant, whereas the Q36A mutant was practically non-functional. IVM only partially rescue the receptor function.

Of all TM1 mutants, the receptor functions were most significantly affected in the P2X4-Y42A mutant that showed enhanced sensitivity to agonists, prolonged deactivation time a reduced I_{max}. IVM treatment did not further sensitize the Y42A mutant function. The EC_{50} values for ATP were identical in the absence and presence of IVM (0.6±0.1 μM) as well as receptor deactivation (τ_{off} = 24±2.9 s in the absence of IVM and 29±4.4 s in the presenceof IVM). The maximum current amplitude was also not enlarged by IVM. It was interesting that mutation of this single TM1 residue, that probably could not contribute directly to the formation of the ATP binding or IVM binding pocket, has such profound effects. Thus we focused on the conserved tyrosine residue at α-position of TM1 ***(Fig. 2)*** across P2X receptors.

Mutant P2X1-Y43A was expressed in the plasma membrane ***(Fig. 6B)*** but was nonfunctional suggesting the importance of this residue in receptor function. The other mutants (P2X2-Y43A, P2X3-Y37A, P2X4-Y42A, P2X7-Y40A) were functional ***(Fig. 6A)***. Deactivation time of P2X2-Y43A mutant was significantly delayed but not so dramatically as for the P2X4-Y42A mutant. The deactivation kinetics of the P2X3-Y37A mutant was biexponential: the mean value of the fast decay component (0.6±0.01s) was comparable with τ_{off} of the P2X3WT, while the slow decay component (34.2±2 s; 36±4%) was comparable with τ_{off} of the P2X4-Y42A mutant. The P2X7-Y40A mutant showed no changes in values of fast deactivation decay τ_{off1} and slow deactivation decay τ_{off2}.

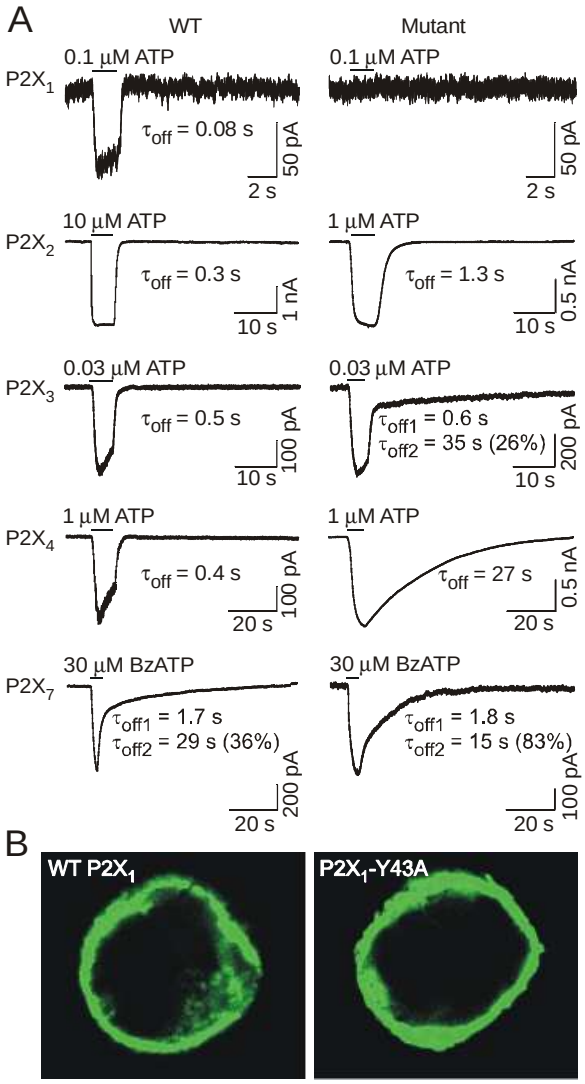

Fig. 6 Effects of replacement of the conserved TM1 tyrosine residue with alanine on the expression and function of P2XRs:

(A) Example records of agonist-induced currents in cells expressing the wild type (WT, *left*) and alanine mutants at α-position (*right*) in TM1 of P2X1R, P2X2R, P2X3R, P2X4R, and P2X7R. Currents were recorded from HEK293 cells using the whole-cell patch clamp recording at holding potential of -60 mV. Horizontal bars indicate the time of ATP or BzATP application. Numbers below traces show deactivation time constant values (τ_{off}) derived from monoexponential fitting of current decay (P2X1R, P2X2R, P2X4R) and biexponential fitting (P2X3R and P2X7R, for which the percentage of slow component (τ_{off2}) contribution to current decay is also shown). (B) Expression pattern of the WT and non-functional P2X1-Y43A mutant in HEK293 cells.

Conserved tyrosine mutants of P2X2R, P2X3R, P2X4R resulted in higher ATP sensitivity with the leftward shifts of EC_{50} values of 20, 10, and 2 fold for P2X2-Y43A, P2X4-Y42A and P2X3-Y37A, respectively ***(Fig. 7A-C)***. In contrast, the P2X7WT and the P2X7-Y40A mutant exhibited equipotent sensitivity to full agonist BzATP ***(Fig. 7D)***.

Mutants P2X2-Y43A, P2X4-Y42A showed differences in the sensitivity to αβ-meATP and the transition from a partial to full agonist for these two receptors ***(Fig. 7A, 7C)***. The P2X7R mutant did not gain sensitivity to partial agonist ATP ***(Fig. 7D)***.

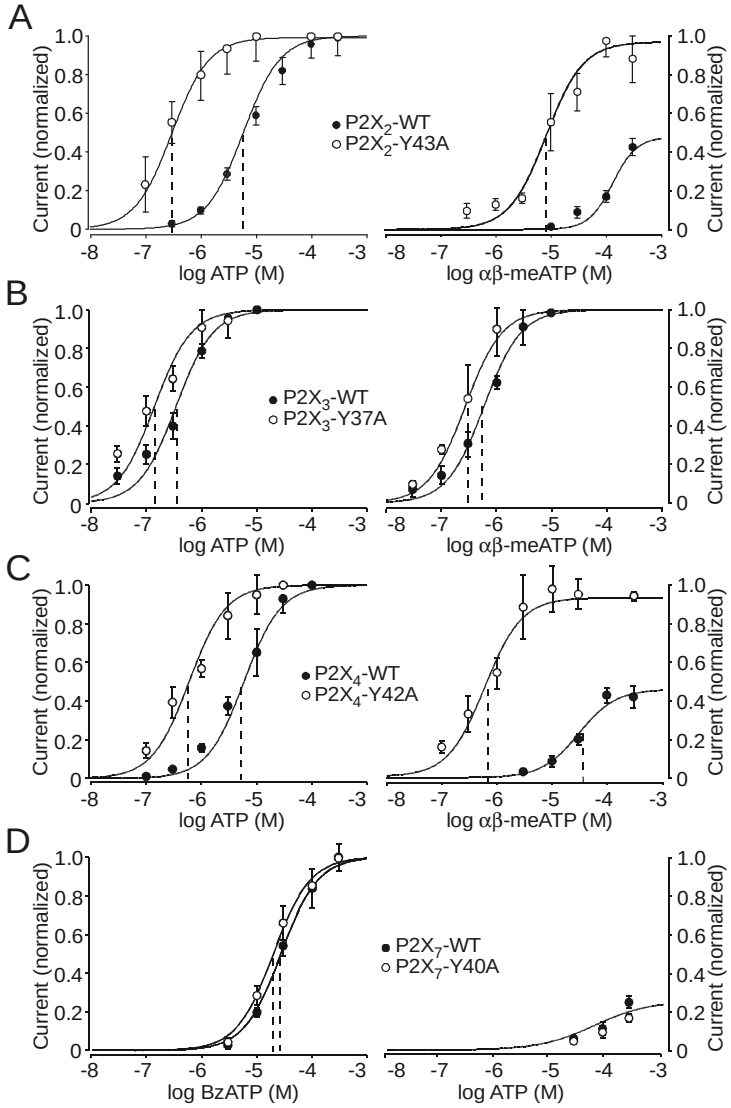

Fig. 7 Effects of replacement of the conserved TM1 tyrosine residue with alanine on the potency of agonists for P2XRs:

Concentration dose-response curves to agonists at WT (●) and TM1 tyrosine to alanine mutants (○) of P2XRs expressed in HEK293 cells. (*Left*) Increase in the sensitivity to ATP in mutants of P2X2R, P2X3R, P2X4R (A-C). The lack of effects of TM1-Tyr mutation on sensitivity to BzATP in P2X7R (D). Current responses were normalized to maximum current induced by 100 μM ATP (P2X2R, P2X3R, P2X4R) and 300 μM BzATP (P2X7R). (*Right*) A leftward shift in the αβmeATP sensitivity of TM1-Tyr mutants of P2X2R, P2X3R, P2X4R (A-C). αβmeATP is a partial agonist for the WT-P2X2R and -P2X4R, its efficacy was measured by comparison with maximum effect of ATP. (D) The lack of effects of this mutation on ATP sensitivity in P2X7R. Each concentration was examined in 5 to 30 different cells. Vertical dashed lines indicate the EC_{50} values.

In conclusion these results suggest that conserved TM1 tyrosine plays important role in the three-dimensional structure of P2XRs required for agonist binding and/or channel gating. The P2X7 receptor tolerates replacement of conserved tyrosine with alanine well suggesting that the binding/gating properties of this receptor differ from the other members of P2XR family. At the P2X4R, replacement of conserved TM1 tyrosine with other amino acids also enhanced the receptor sensitivity to agonist and delayed deactivation in order: Gly > Ile > Ala > Cys > Trp > Phe > Tyr showing that aromatic residue is required at this position for normal receptor function.

We also generated alanine mutants of other aromatic residues at positions β, γ, and δ in the upper part of P2XR-TM1 domains ***(Fig. 2)***: P2X2-F44A, P2X2-Y47A, P2X2-F49A, P2X3-F38A, P2X3-W41A, P2X3-F43A, P2X4-W46A and P2X4-F48A mutants ***(Fig. 8)***.

P2XRs	ATP EC_{50} (μM)	WT/Mutant EC_{50} ratio	ATP I_{max} (nA)	ATP τ_{off} (s)	αβ–meATP EC_{50} (μM)	αβ–meATP efficacy (%)[b]
P2X2R-WT	5.4±0.8	-	2.6±0.2	0.34±0.05	>100	44
P2X2R-F49A	10.8±2.1*	0.5	2.2±0.2	0.44±0.06	>100	32
P2X2R-Y47A	0.82±0.1*	6.6	0.46±0.1*	0.36±0.02	11.8±2*	83
P2X2R-F44A	0.26±0.05*	20	0.44±0,1*	1±0.07*	3.4±1*	95
P2X2R-Y43A	0.28±0.05*	19	0.80±0.1*	1.3±0.1*	8.2±1*	94
P2X2R-Y43F	8.2±1.8	0.7	2.8±0.4	0.47±0.1	>100	65
P2X3R-WT	0.35±0.12	-	1.6±0.2	0.55±0.05	0.59±0.1	100
P2X3R-F43A	0.35±0.2	1	0.9±0.1*	0.75±0.06	0.32±0.2	100
P2X3R-W41A	0,39±0.15	0.9	0.7±0.07*	0.67+±0.08	0,56±15	100
P2X3R-F38A	0.31±0.2	1.1	0.3±0.05*	1.95±0.27*	0.29±0,05	100
P2X3R-Y37A	0.14±0.1*	2.5	1.2±0.2	34.±2* [c]	0.27±0.1	100
P2X4R-WT	4.6±0.3	-	1.6±0.2	0.42±0.03	~57	42
P2X4R-W50A	5.1±1.3	0.9	1.7±0.2	0.35±0.08	~85	24
P2X4R-F48A	4.1±0.5	1.1	1.5±0.8	0.6±0.04	13.4±2.1*	62
P2X4R-W46A	3.0±0.5	0.7	1.0±0.16	0.6±0.1	8.9±1.6*	73
P2X4R-Y42A	0.6±0.1*	7.7	0.6±0.3*	24±2.9*	0.6±0.05*	100
Y42A+V43A	0.9±0.1*	5.4	0.3±0.03*	49±2.6*	0.9±0.3*	100
Y42A+W46A	1.4±0.2*	3.3	1.4±0.3	1.2±0.05*	4.7±2.0*	44
Y42A+F48A	0.3±0.1*	15	0.2±0.03*	54±5*	0.3±0.1*	100
Y42A+W50A	1.6±0.3*	2.8	1.2±0.4	1.6±0.2*	8.3±2.3*	53
Y42A+I39A[a]	n.d.	n.d	0.1±0.05*	n.d.	n.d.	n.d.
Y42A+V35A	0.6±0.1*	7.7	0.4±0.1*	33±4.4*	0.6±0.2*	100
Y42A+G29A	0.4±0.1*	11	0.5±0.1*	34±3.4*	0.4±0.05*	77

Fig. 8 Effects of single- and double-point alanine mutagenesis of aromatic residues in the upper part of TM1 domains on receptor functions of P2X2R, P2X3R, P2X4R:

Data shown are mean±SEM values derived from 5 to 35 cells. (*) P<0.01 between WT and mutants;

[a]1 mM ATP was used to estimate I_{max} for this mutant.
[b]αβme ATP efficacy was calculated as ratio of I_{max} at 300 μM αβmeATP/I_{max} at 100 μM ATP.
[c]τ_{off} value for slow deactivation component contributed with 36±4 % to the current decay.

Alanine substitution of the P2X2R in β-position (P2X2-F44A) caused similar changes of kinetics as observed in the P2X2-Y43A mutant: enhanced sensitivity to ATP and αβ-meATP, prolonged deactivation time. The P2X3R has also an aromatic residue at β-position The P2X3-F38A exhibited prolonged deactivation but no enhancement of sensitivity to ATP. However, the amplitude of ATP-induced current was very low and desensitized fast, thus it was difficult to measure dose-response curve. Results suggest that aromatic residues at β-position of TM1 domain have similar role in P2X2R and P2X3R functions as conserved tyrosine at α-position.

All P2XR have an aromatic residue at γ-position. The P2X2-Y47A mutant shows significantly increased sensitivity to ATP and αβ-meATP and the P2X4-W46A mutant showed increased sensitivity to αβ-meATP and reversed the effects of single Tyr^{42} mutation. The P2X3-W41A mutant showed no changes in sensitivity to agonists or channel deactivation. Thus it is reasonable to conclude that the P2X2R and P2X4R represent a separate subgroup of receptors.

Five of seven P2XR have an aromatic residue at δ-position. Alanine substitution of phenylalanine residues at δ-position did not affect the P2X2R, P2X3R and P2X4R functions. Furthermore, mutation of this residue at the P2X4R did not reverse effects of single Tyr^{42} mutation. In contrast, the effects of P2X4-Y42A mutant were almost completely reversed in double Y42A+W46A and Y42A+W50A mutants that exhibited comparable kinetics with the P2X4-WT receptor ***(Fig. 8, 9)***.

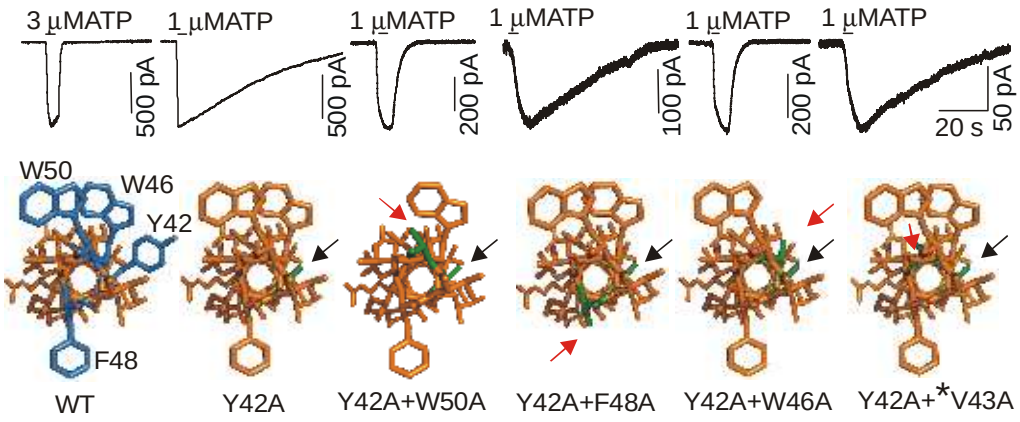

Fig. 9 Effects of replacement of two TM1 aromatic residues with alanine on P2X4R function:

Time-courses of currents by the WT-P2X4R and single point and double-point alanine mutants in response to a brief ATP application (indicated by horizontal bar) (*top*). Dependence of the receptor deactivation on the position of substituted residues in helical model of P2X4R. *Black arrows* indicate alanine substituting conserved tyrosine (*green*) and *red arrows* indicate the second substituting residue (*green*) (aromatic Trp^{46}, Trp^{50} and Phe^{48} or non-aromatic residue Val^{43} (*) present in β positions) (*botoom*).

The helical presentation of TM1 P2X4R indicate that Phe^{48} residue is on the opposite side of molecule than 42, 46, and 50 residues ***(Fig. 5)***. Residue Trp^{50} was identified as IVM-sensitive hit that might face lipid, whereas Tyr^{42} face the pore or most probably the protein-protein interface between two neighboring subunits. Likewise, the ATP binding site in ectodomain is probably located in the inter-subunit pocket (Wilkinson et al., 2006; Marquez-Klaka et al., 2007), indicating that substitution of TM1 aromatic residue at the interface embedded in the membrane might induce far-reaching changes in the ectodomain and affect agonist binding. An alternative explanation would be that aromatic residues at positions 42, 46, and 50 may play a critical role in channel gating.

6. Conclusions

We studied the relationship between the structure and function of the rat purinergic P2X receptors using the patch clamp and molecular biology techniques. We performed cysteine and alanine mutagenesis of TM domains of the P2X4R and using IVM, a specific allosteric modulator, as a lipophilic tool interacting with P2X4R-TMs we tried to identify the IVM-sensitive residues that might face lipids. Simultaneously, the IVM effect was used also as a tool to recognize the secondary structure of TM domains of the P2X4R.

The second part of this work was focused on the aromatic residues in position α, β, γ, δ in the upper part of TM1 domains of the rat P2X1, P2X2, P2X3, P2X4 and P2X7 receptors. We provided a comparative view on the role of these residues in receptor function.

1. We confirmed helical conformation of TM1 and TM2 domains at the P2X4 receptor.

2. Following amino acid residues of TM domains at the P2X4R (Arg^{33}, Gln^{36}, Leu^{40}, Val^{43}, Val^{47}, Trp^{50}, Asn^{338}, Gly^{342}, Leu^{346}, Ala^{349}, Cys^{353}, Ile^{356}) were tolerant to cysteine mutagenesis. These residues might form a binding pocket for IVM and are oriented to lipid bilayer in an open state of the P2X4 channel.

3. Following amino acid residues of TM domains at the P2X4R (Met^{31}, Tyr^{42}, Gly^{45}, Val^{49}, Gly^{340}, Leu^{343}, Ala^{344}, Gly^{347}, Thr^{350}, Asp^{354}, Val^{357}) were identified as substitution-sensitive. They are important for receptor function, map another side of the α-helix of TM domains than IVM-interacting residues and could face the protein or hydrophilic pore.

4. The conserved tyrosine residue at position α in TM1 domain is critical for P2X1R activity as its replacement with alanine resulted in a non-functional receptor. The P2X2R, P2X3R, P2X4R, P2X7R α-mutants were functional. At the P2X2R, P2X3R and P2X4R, this mutation increased sensitivity of receptors to ATP and prolonged deactivation time. This mutation also increased the potency and efficacy of αβ-meATP, a partial agonist, for the P2X2R and the P2X4R.

5. Replacement of conserved tyrosine in the P2X4R with other amino acids enhanced receptor sensitivity to agonists and delayed deactivation in order: Gly > Ile > Ala > Cys > Trp > Phe > Tyr; showing that aromatic residue is required at this position for normal receptor function.

6. Receptor P2X7 tolerates replacement of conserved tyrosine with alanine well suggesting that the binding/gating properties of the P2X7R differ from the other members of P2XR family.

7. Mutation of aromatic TM1 residues at β-position of the P2X2R and the P2X3R, had similar effects on receptor function as replacement of conserved TM1 tyrosine. The effects of the replacement of aromatic residues at γ–position differ in individual P2XRs. The replacement of aromatic residues at δ–position did not affect P2XR function.

8. In the P2X4-Y42A mutant, the replacement of Trp^{46} and Trp^{50} residues restored the receptor functions, whereas mutation of aromatic Phe^{48} residue and non-aromatic Val^{43}, Ile^{39} and Gly^{29} residues was ineffective. It indicates that aromatic residues that face the same wall of TM1 helix as conserved tyrosine play an important role in 3-D structure of P2XRs and their functioning.

7. References

Albers-Schonberg G, Arison BH et al. (1981) Avermectins. Structure determination. *J Am Chem Soc.* **103**:4221-4224.

Brake AJ, Wagenbach MJ et al. (1994) New structural motif for ligand-gated ion channels defined by an ionotropic ATP receptor. *Nature.* **371**:519-523.

Cully DF, Vassilatis DK et al. (1994) Cloning of an avermectin-sensitive glutamate-gated chloride channel from Caenorhabditis elegans. *Nature.* **371**:707-711.

Dent JA, Davis MW et al. (1997) avr-15 encodes a chloride channel subunit that mediates inhibitory glutamatergic neurotransmission and ivermectin sensitivity in Caenorhabditis elegans. *EMBO J.*. **16**:5867-5879.

Egan TM, Haines WR et al. (1998) A domain contributing to the ion channel of ATP-gated P2X2 receptors identified by the substituted cysteine accessibility method. *J Neurosci.* **18**:2350-2359.

Egan TM, Khakh BS (2004) Contribution of Calcium Ions to P2X Channel Responses. *J Neurosci.*. **24**:3413-3420.

Guex N, Peitsch MC (1997) SWISS-MODEL and the Swiss-PdbViewer: An environment for comparative protein modeling. *Electrophoresis.* **18**:2714-2723.

Haines WR, Voigt MM et al. (2001) On the contribution of the first transmembrane domain to whole-cell current through an ATP-gated ionotropic P2X receptor. *J Neurosci* **21**:5885-5892.

Hassinen T, Perakyla M (2001) New energy terms for reduced protein models implemented in an off-lattice force field. *J Comput Chem.* **22**:1229-1242.

Hu X, Gu J, Chen L, HuangPu Y (1998) Studies on the crystal structure of ivermectin (H2B1a) *Yao Xue Xue Bao***. 33**:449-452.

Jiang LH, Kim M et al. (2003) Subunit Arrangement in P2X Receptors. *J Neurosci.* **23**:8903-8910.

Jiang LH, Rassendren F et al. (2001) Amino acid residues involved in gating identified in the first membrane-spanning domain of the rat P2X(2) receptor. *J Biol Chem.* **276**:14902-14908.

Khakh BS, Burnstock G et al. (2001) International union of pharmacology. XXIV. Current status of the nomenclature and properties of P2X receptors and their subunits. *Pharmacol Rev.* **53**:107-118.

Khakh BS, Egan TM (2005). Contribution of transmembrane regions to ATP-gated P2X2 channel permeability dynamics. *J Biol Chem.* **280**:6118-6129.

Khakh BS, Proctor WR et al. (1999) Allosteric control of gating and kinetics at P2X4 receptor channels. *J Neurosci.* **19**:7289-7299.

Krause RM, Buisson B et al. (1998) Ivermectin: a positive allosteric effector of the alpha7 neuronal nicotinic acetylcholine receptor. *Mol Pharmacol.* **53**:283-294.

Krusek J, Zemkova H (1994) Effect of ivermectin on gamma-aminobutyric acid-induced chloride currents in mouse hippocampal embryonic neurones. *J Pharmacol.* **259**:121-128.

Li M, Chang TH et al. (2008) Gating the pore of P2X receptor channels. *Nat Neurosci.* **11**:883-887.

Li Z, Migita K et al. (2004) Gain and loss of channel function by alanine substitutions in the transmembrane segments of the rat ATP-gated P2X2 receptor. *J Neurosci.* **24**:7378-7386.

Marquez-Klaka B, Rettinger J et al. (2007) Identification of an intersubunit cross-link between substituted cysteine residues located in the putative ATP binding site of the P2X1 receptor. *J Neurosci.* **27**:1456-1466.

Migita K, Haines WR et al. (2001) Polar residues of the second transmembrane domain influence cation permeability of the ATP-gated P2X2 receptor. *J Biol Chem.* **276**:30934-30941.

Nicke A, Baumert HG et al. (1998) P2X1 and P2X3 receptors form stable trimers: a novel structural motif of ligand-gated ion channels. *Embo J.* **17**:3016-3028.
North RA (2002) Molecular Physiology of P2X Receptors. *Physiol Rev.* **82**:1013-1067.
Priel A, Silberberg SD (2004) Mechanism of ivermectin facilitation of human P2X4 receptor channels. *J Gen Physiol.* **123**:281-293.
Rassendren F, Buell G et al. (1997) Identification of amino acid residues contributing to the pore of a P2X receptor. *Embo J.* **16**:3446-3454.
Samways DS, Egan TM (2007) Acidic amino acids impart enhanced Ca2+ permeability and flux in two members of the ATP-gated P2X receptor family. *J Gen Physiol.* **129**:245-256.
Samways DS, Migita K et al. (2008) On the role of the first transmembrane domain in cation permeability and flux of the ATP-gated P2X2 receptor. *J Biol Chem.* **283**:5110-5117.
Shan Q, Haddrill JL, Lynch JW (2001) Ivermectin, an unconventional agonist of the glycine receptor chloride channel. *J Biol Chem.* **276**:12556-12564.
Sigel E, Baur R (1987) Effect of avermectin B1a on chick neuronal gamma-aminobutyrate receptor channels expressed in Xenopus oocytes. *Mol Pharmacol.* **32**:749-752.
Silberberg SD, Chang TH, Swartz KJ (2005) Secondary structure and gating rearrangements of transmembrane segments in rat P2X4 receptor channels. *J Gen Physiol.* **125**:347-359.
Silberberg SD, Li M, Swartz KJ (2007) Ivermectin Interaction with transmembrane helices reveals widespread rearrangements during opening of P2X receptor channels. *Neuron.* **54**:263-274.
Valera S, Hussy N et al. (1994) A new class of ligand-gated ion channel defined by P2x receptor for extracellular ATP. *Nature.* **371**:516-519.
Wilkinson WJ, Jiang LH et al. (2006) Role of ectodomain lysines in the subunits of the heteromeric P2X2/3 receptor. *Mol Pharmacol.* **70**:1159-1163.
Yan Z, Liang Z et al. (2005) Molecular Determinants of the Agonist Binding Domain of a P2X Receptor Channel. *Mol Pharmacol.* **67**:1078-1088.
Zemkova H, Yan Z et al. (2007) Role of Aromatic and Charged Ectodomain Residues in the P2X4 Receptor Functions. *J Neurochem.* **102**:1139-1150.

8. List of publications

Publications related to theme:

Jindrichova M, Vavra V, Obsil T, Stojilkovic SS, Zemkova H (2008) Functional relevance of aromatic residues in the first transmembrane domain of P2X receptors. *J Neurochem.*, in press. (IF 4.451)

Jelinkova I, Vavra V, Jindrichova M, Obsil T, Zemkova HW, Zemkova H, Stojilkovic SS (2008) Identification of P2X(4) receptor transmembrane residues contributing to channel gating and interaction with ivermectin. *Pflugers Arch.* **456**:939-950. (IF 3.842)

Zemkova H, Balik A, Jindrichova M, Vavra V (2008) Molecular Structure of Purinergic P2X Receptors and their Expression in the Hypothalamus and Pituitary. *Physiol Res.* **57**:S23-S38. (IF 1.505)

Other publications:

Balik A, Jindrichova M, Bhattacharyya S, Zemkova H (2008) GnRH-I and GnRH-II--induced calcium signaling and hormone secretion in neonatal rat gonadotrophs. *Physiol Res.* Nov 4, in press. (IF 1.505)

Abstracts in impact journals:

Jindrichova M, Vavra V, Zemkova H (2008) Differential effect of tyrosine to alanine substitution in the first transmembrane domain in P2X7 and other P2X subunits. *Physiol Res*. **57**:78P-79P. (IF 1.505)

Jindrichova M, Vavra V, Obsil T, Stojilkovic SS, Zemkova H (2008) A role of conserved tyrosine in the first transmembrane domain in purinergic P2X receptor function. *Purinergic Signal.* **4**:S199-S200.

Jelinkova I, Jindrichova M, Vavra V, Zemkova H (2006) Ivermectin sensitivity of heteromeric P2X4+P2X1 and P2X4+P2X6 purinergic receptors. *FEBS Journal.* **273**:330. (IF 3.396)